Interpolation lattices for hyperbolic cross trigonometric polynomials

Lutz Kämmerer* Stefan Kunis*‡ Daniel Potts*

Sparse grid discretisations allow for a severe decrease in the number of degrees of freedom for high dimensional problems. Recently, the corresponding hyperbolic cross fast Fourier transform has been shown to exhibit numerical instabilities already for moderate problem sizes. In contrast to standard sparse grids as spatial discretisation, we propose the use of oversampled lattice rules known from multivariate numerical integration. This allows for the highly efficient and perfectly stable evaluation and reconstruction of trigonometric polynomials using only one ordinary FFT. Moreover, we give numerical evidence that reasonable small lattices exist such that our new method outperforms the sparse grid based hyperbolic cross FFT for realistic problem sizes.

Key words and phrases : trigonometric approximation, hyperbolic cross, sparse grid, lattice rule, fast Fourier transform

2000 AMS Mathematics Subject Classification : 65T40, 42B05, 65D30.

1 Introduction

A straightforward discretisation of problems in d spatial dimensions with 2^n grid points in each coordinate leads to an exponential growth 2^{dn} in the number of degrees of freedom. Even an efficient algorithm like the d-dimensional fast Fourier transform (FFT) uses $C2^{dn}dn$ floating point operations. This is labelled as the curse of dimensions and the use of sparsity has become a very popular tool in such situations. For moderately high dimensional problems the use of sparse grids and the approximation on hyperbolic crosses has led to problems of total size $C_d 2^n n^{d-1}$. Moreover, the approximation rate hardly deteriorates for functions in an appropriate scale of spaces of dominating mixed smoothness, see e.g. [23, 26, 19, 18, 22, 2, 20, 24]. The FFT has been adapted to this thin discretisation as hyperbolic cross fast Fourier transform (HCFFT), which uses $C_d 2^n n^d$ floating point operations, in [1, 9, 7]. See also [6] for a recent generalisation to arbitrary spatial sampling nodes and [10] for a more accurate scheme for functions of low regularity. However, these classical sparse grid discretisations are numerically unstable as shown in [11].

*Chemnitz University of Technology, Faculty of Mathematics, {kaemmerer,kunis,potts}@mathematik.tu-chemnitz.de

‡Helmholtz Zentrum München, Institute for Biomathematics and Biometry

On the other hand, lattice rules are well known for the integration of functions of many variables, see e.g. [21] and references therein. The numerical integration of trigonometric polynomials of certain total degree or with Fourier coefficients supported on a hyperbolic cross have been studied recently in [4] and [14], respectively. In particular, the authors of [3] were able to search for so called rank-1 integration lattices in an effective way.

In this paper, we consider rank-1 lattice rules as spatial discretisation for the hyperbolic cross FFT. The evaluation of trigonometric polynomials, i.e., the mapping from the hyperbolic cross in frequency domain to the lattice in spatial domain reduces to a single one dimensional FFT and thus can be computed very efficiently and stable. For the inverse transform, mapping the samples of a trigonometric polynomial to its Fourier coefficients on the hyperbolic cross, we show which necessary and sufficient conditions allow for unique and stable reconstruction. In conjunction with numerical found lattices, we show that this new method outperforms the classical hyperbolic cross FFT for realistic problem sizes.

The paper is organised as follows: After introducing the necessary notation and collecting basic facts about hyperbolic crosses, we state the evaluation and reconstruction problem formally. In Section 3, we define the rank-1 lattices and show how this simplifies the evaluation problem. The reconstruction problem is divided into a qualitative and a quantitative question, i.e., we ask for uniqueness and stability, respectively. After a first example, we show that unique reconstruction is possible even for a number of samples equal to the dimension of the underlying space of trigonometric polynomials. However, this scheme is numerically unstable. Asking for perfectly stable reconstruction is equivalent to asking for orthogonal columns of the corresponding Fourier matrix. We show that this is possible only for so-called integer rank-1 lattices and in general only for a number of samples which scales almost quadratically in the dimension of the underlying space of trigonometric polynomials. Besides the usage of known integration lattices for the reconstruction problem, we search for appropriate rank-1 lattices of minimal cardinality. In this context, we consider generating vectors of Korobov form which have some useful properties and allow for a reduction of computational costs for searching. All theoretical results are illustrated by numerical experiments in Section 4 and we conclude our findings in Section 5.

2 Prerequisite

Throughout this paper let the spatial dimension $d \in \mathbb{N}$ and a refinement $n \in \mathbb{N}_0$ be given. We denote by $\mathbb{T}^d \cong [0,1)^d$ the d-dimensional torus and consider Fourier series $f : \mathbb{T}^d \to \mathbb{C}$, $f(\boldsymbol{x}) = \sum_{\boldsymbol{k}\in\mathbb{Z}^d} \hat{f}_{\boldsymbol{k}} \mathrm{e}^{2\pi \mathrm{i} \boldsymbol{k}\cdot\boldsymbol{x}}$ with Fourier coefficients $\hat{f}_{\boldsymbol{k}} \in \mathbb{C}$. The space of trigonometric polynomials $\Pi_{\boldsymbol{j}}$, $\boldsymbol{j} \in \mathbb{N}_0^d$, consists of all such series with Fourier coefficients supported on $\hat{G}_{\boldsymbol{j}} = \times_{l=1}^d \hat{G}_{j_l}$, $\hat{G}_j = \mathbb{Z} \cap (-2^{j-1}, 2^{j-1}]$, i.e., $f : \mathbb{T}^d \to \mathbb{C}$,

$$f(\boldsymbol{x}) = \sum_{\boldsymbol{k}\in\hat{G}_{\boldsymbol{j}}} \hat{f}_{\boldsymbol{k}} \mathrm{e}^{2\pi \mathrm{i} \boldsymbol{k}\cdot\boldsymbol{x}}.$$

A well adapted spatial discretisation of trigonometric polynomials relies on the full spatial grid $G_{\boldsymbol{j}} = \times_{l=1}^d G_{j_l}$, $G_j = 2^{-j}(\mathbb{Z} \cap [0, 2^j))$. If all refinements are equally set to $j_l = n$, $l = 1, \ldots, d$, we write $\hat{G}_n^d$ and G_n^d instead of $\hat{G}_{(n,\ldots,n)^T}$ and $G_{(n,\ldots,n)^T}$, respectively. Note that these grids have 2^{dn} degrees of freedom in frequency as well as in spatial domain.

2.1 Hyperbolic crosses

For functions of appropriate smoothness, it is much more effective to restrict the frequency domain to hyperbolic crosses. To this end, we introduce the *dyadic hyperbolic cross*

$$H_n^d := \bigcup_{\substack{\boldsymbol{j}\in\mathbb{N}_0^d \\ \|\boldsymbol{j}\|_1=n}} \hat{G}_{\boldsymbol{j}} = \{\boldsymbol{k}\in\hat{G}_{\boldsymbol{j}} : \boldsymbol{j}\in\mathbb{N}_0^d,\ \|\boldsymbol{j}\|_1=n\} \qquad \subset \hat{G}_n^d \subset \mathbb{Z}^d, \tag{2.1}$$

see Figure 2.1(a) and furthermore we define for $0<\gamma\le 1$ and $n>0$, $2^n\in\mathbb{N}$, the *symmetric hyperbolic cross*

$$\tilde{H}_n^{d,\gamma} := \{\boldsymbol{k}\in\mathbb{Z}^d : \prod_{s=1}^d \max\left(1, \frac{|k_s|}{\gamma}\right) \le 2^n\} \tag{2.2}$$

see Figure 2.1(b) and (c). $\tilde{H}_n^{d,\gamma}$ are also called *weighted Zaremba crosses*, see e.g. [3], and simply *Zaremba crosses* for $\gamma=1$, cf. [25], respectively. We have the following relations

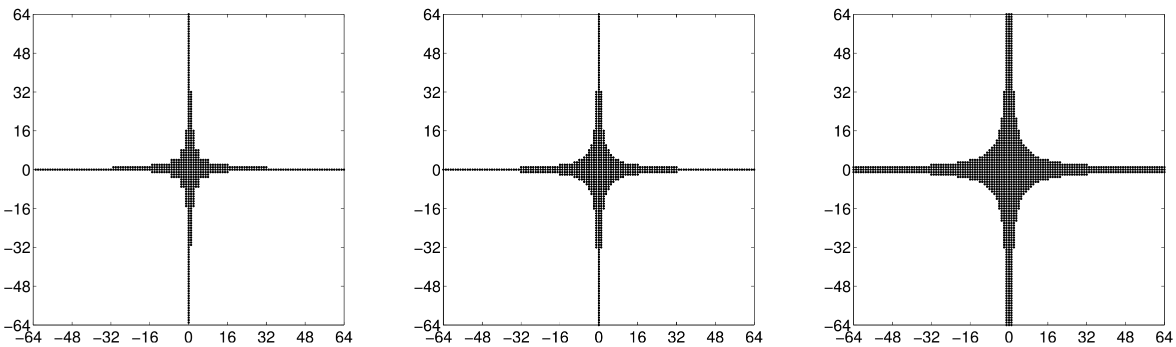

(a) Dyadic hyperbolic cross H_7^2. (b) Symmetric hyperbolic cross $\tilde{H}_7^{2,\frac{1}{2}}$. (c) Symmetric hyperbolic cross $\tilde{H}_6^{2,1}$.

Figure 2.1: Two dimensional hyperbolic crosses.

between the dyadic and the symmetric hyperbolic crosses.

Lemma 2.1. *For $d,n\in\mathbb{N}$, we have the inclusions*

$$H_n^d \subset \tilde{H}_n^{d,\frac{1}{2}} \subset \tilde{H}_{n-1}^{d,1} \subset \tilde{H}_{n-1+d}^{d,\frac{1}{2}} \subset H_{n-1+2d}^d,$$

where each individual inclusion is best possible.

Proof. For subsequent use, set $\mathcal{I}_{\boldsymbol{k}} := \{s\in\{1,\ldots,d\} : k_s\neq 0\}$, $\boldsymbol{k}\in\mathbb{Z}^d$. Regarding the first assertion, let $\boldsymbol{k}\in H_n^d$ and $\boldsymbol{j}\in\mathbb{N}_0^d$, $\|\boldsymbol{j}\|_1=n$, with $\boldsymbol{k}\in\hat{G}_{\boldsymbol{j}}$ be given. Then we infer $|k_s|\le 2^{j_s-1}$ for $s\in\mathcal{I}_{\boldsymbol{k}}$ and $\boldsymbol{k}\in\tilde{H}_n^{d,\frac{1}{2}}$ since $\prod_{s=1}^d \max(1,2|k_s|) = \prod_{s\in\mathcal{I}_{\boldsymbol{k}}}\max(1,2|k_s|) \le \prod_{s\in\mathcal{I}_{\boldsymbol{k}}} 2^{j_s} \le 2^n$.

Secondly, we have $\boldsymbol{0}=(0,\ldots,0)^\top\in\tilde{H}_n^{d,\frac{1}{2}}\cap\tilde{H}_{n-1}^{d,1}$ and $\boldsymbol{k}\in\tilde{H}_n^{d,\frac{1}{2}}\setminus\{\boldsymbol{0}\}$ implies $\mathcal{I}_{\boldsymbol{k}}\neq\emptyset$ and thus $\boldsymbol{k}\in\tilde{H}_{n-1}^{d,1}$ since

$$2^n \ge \prod_{s=1}^d \max(1,2|k_s|) = \prod_{s\in\mathcal{I}_{\boldsymbol{k}}} 2|k_s| = 2^{|\mathcal{I}_{\boldsymbol{k}}|}\prod_{s\in\mathcal{I}_{\boldsymbol{k}}}|k_s| \ge 2\prod_{s=1}^d \max(1,|k_s|).$$

The third inclusion is a consequence of $\prod_{s=1}^d \max(1, 2|k_s|) \le \prod_{s=1}^d 2\max(1, |k_s|) \le 2^{n-1+d}$. For notational convenience, we prove the last assertion in its equivalent form $\tilde{H}_n^{d,\frac{1}{2}} \subset H_{n+d}^d$ for $n \ge d$. For $\boldsymbol{k} \in \tilde{H}_n^{d,\frac{1}{2}}$ choose $\boldsymbol{j} \in \mathbb{N}_0^d$ such that $k_s \in \hat{G}_{j_s} \setminus \hat{G}_{j_s-1}$, $s \in \mathcal{I}_{\boldsymbol{k}}$, and $j_s = 0$ else. This yields

$$2^{\|\boldsymbol{j}\|_1 - 2|\mathcal{I}_{\boldsymbol{k}}|} \le \prod_{s \in \mathcal{I}_{\boldsymbol{k}}} |k_s| \quad \text{and} \quad 2^{\|\boldsymbol{j}\|_1 - d} \le 2^{\|\boldsymbol{j}\|_1 - |\mathcal{I}_{\boldsymbol{k}}|} \le \prod_{s \in \mathcal{I}_{\boldsymbol{k}}} 2|k_s| \le 2^n$$

from which $\|\boldsymbol{j}\|_1 \le n + d$ and thus $\boldsymbol{k} \in \hat{G}_{\boldsymbol{j}} \subset H_{n+d}^d$ follows.

Note that all inclusions are best possible as $\boldsymbol{k}_1 = (2^{n-1}, 0, \ldots, 0) \in H_n^d \cap \tilde{H}_n^{d,\frac{1}{2}} \cap \tilde{H}_{n-1}^{d,1}$ and $\boldsymbol{k}_2 = (-2^{n-1}, -1, \ldots, -1) \in \tilde{H}_{n-1}^{d,1} \cap \tilde{H}_{n-1+d}^{d,\frac{1}{2}} \cap H_{n-1+2d}^d$ show. ■

We have for fixed dimension d that $|H_n^d| = \frac{2^n n^{d-1}}{2^{d-1}(d-1)!} + \mathcal{O}(2^n n^{d-2})$, cf. [9], and so the above inclusions also yield $|\tilde{H}_n^{d,\gamma}| = C_d 2^n n^{d-1}$. Moreover note, that including so-called additional logarithmic smoothness terms in (2.2) one can define "energy based" hyperbolic crosses that remove the term n^{d-1}, see [2, pp. 31-35].

We denote by Π_n^d and $\tilde{\Pi}_n^{d,\gamma}$ the trigonometric polynomials on the dyadic hyperbolic cross $f : \mathbb{T}^d \to \mathbb{C}$,

$$f(\boldsymbol{x}) = \sum_{\boldsymbol{k} \in H_n^d} \hat{f}_{\boldsymbol{k}} \, \mathrm{e}^{2\pi \mathrm{i} \boldsymbol{k} \cdot \boldsymbol{x}},$$

and the trigonometric polynomials on the symmetric hyperbolic cross $f : \mathbb{T}^d \to \mathbb{C}$,

$$f(\boldsymbol{x}) = \sum_{\boldsymbol{k} \in \tilde{H}_n^{d,\gamma}} \hat{f}_{\boldsymbol{k}} \, \mathrm{e}^{2\pi \mathrm{i} \boldsymbol{k} \cdot \boldsymbol{x}},$$

respectively. With these thin discretisations in frequency domain, we are concerned with the evaluation of trigonometric polynomials at sampling nodes and the inverse problem of reconstructing a trigonometric polynomial from its samples. In view of Lemma 2.1, all statements that follow might be adapted to the symmetric hyperbolic crosses. Our evaluation and reconstruction problems read as follows

i) given Fourier coefficients $\hat{\boldsymbol{f}} = \left(\hat{f}_{\boldsymbol{k}}\right)_{\boldsymbol{k} \in H_n^d} \in \mathbb{C}^{|H_n^d|}$ and a set of sampling nodes $\mathcal{X} = \{\boldsymbol{x}_j \in \mathbb{T}^d : j = 0, \ldots, M-1\}$, evaluate the trigonometric polynomial $f(\boldsymbol{x}_j)$, $j = 0, \ldots, M-1$,

ii) construct a set of sampling nodes $\mathcal{X} \subset \mathbb{T}^d$ with small cardinality M which allows for the stable reconstruction of all trigonometric polynomials $f \in \Pi_n^d$, represented by their Fourier coefficients $\hat{\boldsymbol{f}} \in \mathbb{C}^{|H_n^d|}$, from the sample values $f(\boldsymbol{x}_j)$, $j = 0, \ldots, M-1$.

For notational convenience let the *Fourier matrix* and the *index matrix*

$$\boldsymbol{A} := \left(\mathrm{e}^{2\pi \mathrm{i} \boldsymbol{k} \cdot \boldsymbol{x}}\right)_{\boldsymbol{x} \in \mathcal{X}, \boldsymbol{k} \in H_n^d}, \qquad \boldsymbol{H} \in \mathbb{Z}^{|H_n^d| \times d},\ h_{\boldsymbol{k},s} = k_s,\ \boldsymbol{k} \in H_n^d,\ s \in \{1, \ldots, d\},$$

be given.

3 Lattices

An introduction to lattices, in particular their use for the efficient integration of functions of many variables can be found in [21]. In contrast to general lattices which are spanned by several vectors, we only consider so-called rank-1 lattices. This simplifies the evaluation of trigonometric polynomials dramatically and allows for several necessary and sufficient conditions for unique or stable reconstruction. For given $M \in \mathbb{N}$ and $\boldsymbol{r} \in \mathbb{R}^d$, we define the *rank-1 lattice*

$$\mathcal{X} := \{\boldsymbol{x}_j = j\boldsymbol{r} \mod 1,\ j = 0, \ldots, M-1\} \subset \mathbb{T}^d.$$

Hence, evaluation problem i) from above reads as

$$f(\boldsymbol{x}_j) = \sum_{\boldsymbol{k}\in H_n^d} \hat{f}_{\boldsymbol{k}} \mathrm{e}^{2\pi\mathrm{i}\boldsymbol{k}\cdot\boldsymbol{x}_j} = \sum_{\boldsymbol{k}\in H_n^d} \hat{f}_{\boldsymbol{k}} \mathrm{e}^{2\pi\mathrm{i}j\boldsymbol{k}\cdot\boldsymbol{r}} = \sum_{y\in\mathcal{Y}} \hat{g}_y \mathrm{e}^{2\pi\mathrm{i}jy}, \qquad j = 0, \ldots, M-1, \tag{3.1}$$

with some set $\mathcal{Y} = \{\boldsymbol{k} \cdot \boldsymbol{r} \mod 1 : \boldsymbol{k} \in H_n^d\} \subset \mathbb{T}$ and the aliased coefficients

$$\hat{g}_y = \sum_{\boldsymbol{k}\cdot\boldsymbol{r}=y \mod 1} \hat{f}_{\boldsymbol{k}}.$$

This is a one dimensional adjoint nonequispaced fast Fourier transform, see e.g. [13], which takes $\mathcal{O}(M \log M + |\log \varepsilon||H_n^d|)$ floating point operations, where ε is the user specified target accuracy. Moreover, for given $M \in \mathbb{N}$ and $\boldsymbol{z} \in \mathbb{Z}^d$, we define the *integer rank-1 lattice*

$$\mathcal{X} := \{\boldsymbol{x}_j = j\boldsymbol{z}/M \mod 1,\ j = 0, \ldots, M-1\} \subset \mathbb{T}^d.$$

Analogously, we obtain for the evaluation problem i) a one dimensional fast Fourier transform of length M and thus total complexity $\mathcal{O}(M \log M + |H_n^d|)$. We stress on the fact that, in both cases, the computational complexity depends only on M and $|H_n^d|$ but not on the spatial dimension d itself.

Concerning the reconstruction problem ii), i.e., the construction of good lattices, we have

- ii-a) the *qualitative* question under which assumption the lattice allows for unique reconstruction or equivalently $\boldsymbol{A}$ has full column rank $|H_n^d|$,
- ii-b) the *quantitative* question under which assumption the lattice allows for stable reconstruction or in the strictest sense $\boldsymbol{A}^*\boldsymbol{A} = M\boldsymbol{I}$.

In particular, the condition in ii-b) allows for the computation of all Fourier coefficients by means of a one dimensional fast Fourier transform of length M instead of solving some system of linear equations.

Lemma 3.1. *Let $n, d \in \mathbb{N}$. For rank-1 lattices with lattice size $M \geq |H_n^d|$, the matrix $\boldsymbol{A} \in \mathbb{C}^{M\times|H_n^d|}$ has full column rank $|H_n^d|$ if and only if the entries of the vector*

$$\boldsymbol{y} = (y_{\boldsymbol{k}})_{\boldsymbol{k}\in H_n^d} = \boldsymbol{H}\boldsymbol{r} \mod 1$$

are distinct.

Proof. Let $y_{\boldsymbol{k}} = y_{\boldsymbol{l}}$ for some $\boldsymbol{k}, \boldsymbol{l} \in H_n^d$, $\boldsymbol{k} \neq \boldsymbol{l}$, then obviously, the $\boldsymbol{k}$th and $\boldsymbol{l}$th column of the Fourier matrix $\boldsymbol{A}$ coincide, i.e.,

$$\mathrm{e}^{2\pi \mathrm{i} \boldsymbol{k} \cdot j \boldsymbol{r}} = \mathrm{e}^{2\pi \mathrm{i} j y_{\boldsymbol{k}}} = \mathrm{e}^{2\pi \mathrm{i} j y_{\boldsymbol{l}}} = \mathrm{e}^{2\pi \mathrm{i} \boldsymbol{l} \cdot j \boldsymbol{r}}, \qquad j = 0, \ldots, M-1.$$

On the contrary, we only consider the first $|H_n^d|$ rows of the Fourier matrix $\boldsymbol{A}$, i.e.,

$$\tilde{\boldsymbol{A}} = (\mathrm{e}^{2\pi \mathrm{i} \boldsymbol{k} \cdot j \boldsymbol{r}})_{j=0,\ldots,|H_n^d|-1; \boldsymbol{k} \in H_n^d} = \left((\mathrm{e}^{2\pi \mathrm{i} y_{\boldsymbol{k}}})^j \right)_{j=0,\ldots,|H_n^d|-1; \boldsymbol{k} \in H_n^d}.$$

The square matrix $\tilde{\boldsymbol{A}}$ is the adjoint of a Vandermonde matrix with distinct nodes $z_{\boldsymbol{k}} = \mathrm{e}^{2\pi \mathrm{i} y_{\boldsymbol{k}}} \in \mathbb{C}$, $\boldsymbol{k} \in H_n^d$, and thus invertible. ■

Example 3.2. [A minimal and unstable lattice] Let $n, d \in \mathbb{N}$. Due to the fact that $H_n^d \subset \hat{G}_n^d$, we might choose the rank-1 lattice of size $M = |H_n^d|$ with generating vector

$$\boldsymbol{r} = (r, r^2, \ldots, r^d)^\top, \qquad r = 2^{-n}, \tag{3.2}$$

which yields for $\boldsymbol{y} = \boldsymbol{H}\boldsymbol{r}$ the distinct entries

$$y_{\boldsymbol{k}} = \boldsymbol{k} \cdot \boldsymbol{r} = \sum_{s=1}^{d} 2^{-sn} k_s, \qquad 2^{-sn} k_s \in 2^{-sn} \hat{G}_n.$$

Thus, Lemma 3.1 assures an invertible Fourier matrix $\boldsymbol{A}$, i.e., the reconstruction problem allows for a unique solution. However, Figure 3.1 shows that this lattice covers only part of the torus. We show that this leads to a highly unstable reconstruction problem by giving a lower bound on the condition number of the associated Fourier matrix $\boldsymbol{A}$.

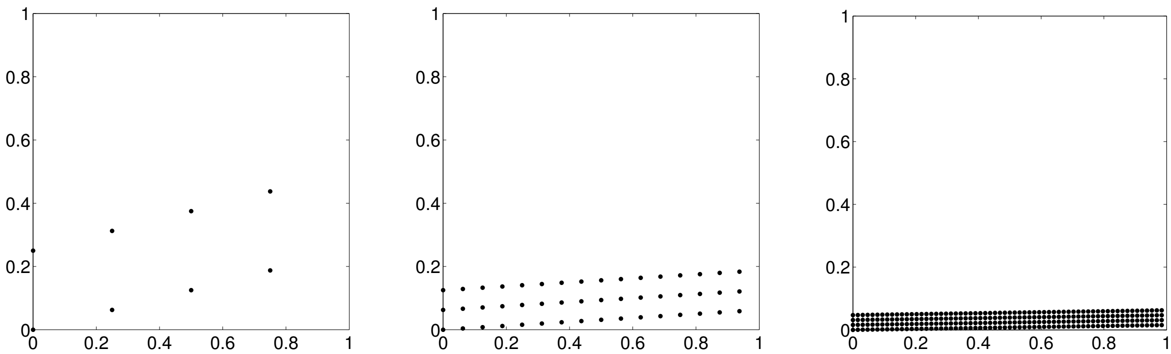

(a) $M = |H_2^2|$, $\boldsymbol{z} = (2^{-2}, 2^{-4})^\top$. (b) $M = |H_4^2|$, $\boldsymbol{z} = (2^{-4}, 2^{-8})^\top$. (c) $M = |H_6^2|$, $\boldsymbol{z} = (2^{-6}, 2^{-12})^\top$.

Figure 3.1: Two-dimensional minimal and unstable lattices for refinements 2, 4 and 6.

For dimension $d = 2$ and refinement $n > 2$, consider the constant function $e(\boldsymbol{x}) = 1$ which has the only nonzero Fourier coefficient at $\boldsymbol{k} = \boldsymbol{0}$, i.e., $\hat{\boldsymbol{e}} \in \mathbb{C}^{|H_n^2|}$, $\hat{e}_{\boldsymbol{k}} = \delta_{\boldsymbol{k}}$. We obtain

$$\|\boldsymbol{A}\|_2^2 \geq \frac{\|\boldsymbol{A}\hat{\boldsymbol{e}}\|_2^2}{\|\hat{\boldsymbol{e}}\|_2^2} = |H_n^2|.$$

For the norm of the inverse Fourier matrix $\boldsymbol{A}^{-1}$, we use that the "Fejér kernel"

$$f(\boldsymbol{x}) = f(x_1, x_2) = \frac{1}{2^{n-1}} \left(\frac{\sin 2^{n-1} \pi x_2}{\cos \pi x_2} \right)^2$$

is localised with respect to the spatial variable x_2 and its Fourier coefficients are supported on one axis of the hyperbolic cross. Straightforward calculation shows $\|\hat{\boldsymbol{f}}\|_2^2 = \|f\|_2^2 \geq \frac{1}{3}2^n$. Since the above lattice fulfils $\mathcal{X} \subset [0,1) \times [0, M2^{-2n}) \subset [0,1) \times [0, \frac{5}{16})$, $n \geq 2$, we estimate $|f(\boldsymbol{x})| \leq 2^{3-n}$ for $\boldsymbol{x} \in \mathcal{X}$ and conclude

$$\|\boldsymbol{A}^{-1}\|_2^2 \geq \frac{\|\hat{\boldsymbol{f}}\|_2^2}{\|\boldsymbol{A}\hat{\boldsymbol{f}}\|_2^2} \geq \frac{2^{3n}}{192|H_n^2|} \quad \text{and finally} \quad \mathrm{cond}_2\boldsymbol{A} = \|\boldsymbol{A}\|_2\|\boldsymbol{A}^{-1}\|_2 \geq \frac{2^{\frac{3n}{2}}}{14}.$$

We note in passing that this lower bound can be improved by stronger localised kernels and that analogous estimates follow for higher spatial dimensions. $\square$

Lemma 3.3. *Let $n, d \in \mathbb{N}$, the sampling set $\mathcal{X}$ be a rank-1 lattice generated by the vector $\boldsymbol{z} \in \mathbb{R}^d$ and the vector $\boldsymbol{H}\boldsymbol{z} \mod M$ contain distinct entries only. Then*

$$\boldsymbol{A}^*\boldsymbol{A} = M\boldsymbol{I} \quad \textit{if and only if} \quad \mathcal{X} \textit{ is an } \text{integer} \textit{ rank-1 lattice.}$$

Proof. Clearly, the entries of the matrix fulfil

$$(\boldsymbol{A}^*\boldsymbol{A})_{\boldsymbol{k},\boldsymbol{l}} = \sum_{j=0}^{M-1} \mathrm{e}^{2\pi\mathrm{i}j\frac{(\boldsymbol{k}-\boldsymbol{l})\cdot\boldsymbol{z}}{M}} = \begin{cases} M, & \text{for } (\boldsymbol{k}-\boldsymbol{l})\cdot\boldsymbol{z} = 0 \mod M \\ \frac{\mathrm{e}^{2\pi\mathrm{i}(\boldsymbol{k}-\boldsymbol{l})\cdot\boldsymbol{z}}-1}{\mathrm{e}^{2\pi\mathrm{i}\frac{(\boldsymbol{k}-\boldsymbol{l})\cdot\boldsymbol{z}}{M}}-1} & \text{else,} \end{cases}$$

from which the assertion for the principal diagonal of $\boldsymbol{A}^*\boldsymbol{A}$ follows. Because of $\mathbb{Z} \ni (\boldsymbol{k}-\boldsymbol{l})\cdot\boldsymbol{z} \neq 0 \mod M$ for $\boldsymbol{k}, \boldsymbol{l} \in H_n^d$ with $\boldsymbol{k} \neq \boldsymbol{l}$ and $\boldsymbol{z} \in \mathbb{Z}^d$ with distinct entries of $\boldsymbol{H}\boldsymbol{z} \mod M$, we get $\boldsymbol{A}^*\boldsymbol{A} = M\boldsymbol{I}$.

Moreover, hyperbolic crosses of refinements $n \geq 1$ contain at least the origin $\boldsymbol{k}_0 = (0,\ldots,0)^\top$ and the unit vectors $\boldsymbol{k}_1 = (1,0,\ldots,0)^\top, \ldots, \boldsymbol{k}_d = (0,\ldots,0,1)^\top$. Hence for $z_s \in \mathbb{R} \setminus \mathbb{Z}$, $s \in \{1,\ldots,d\}$, the entry $(\boldsymbol{A}^*\boldsymbol{A})_{\boldsymbol{k}_0,\boldsymbol{k}_s} \neq 0$ and so $\boldsymbol{A}^*\boldsymbol{A} \neq M\boldsymbol{I}$. $\blacksquare$

Example 3.4. [Refinement $n = 1$ and large spatial dimension d] The hyperbolic cross H_1^d contains the origin $\boldsymbol{k}_0 = (0,\ldots,0)^\top$ and the unit vectors $\boldsymbol{k}_1 = (1,0,\ldots,0)^\top, \ldots, \boldsymbol{k}_d = (0,\ldots,0,1)^\top$. Thus, the associated index matrix $\boldsymbol{H} \in \mathbb{Z}^{(d+1)\times d}$ fulfils

$$\boldsymbol{H}\boldsymbol{z} = \begin{pmatrix} \boldsymbol{0} \\ \boldsymbol{I}_d \end{pmatrix} \boldsymbol{z} = \begin{pmatrix} 0 \\ \boldsymbol{z} \end{pmatrix}, \qquad \text{for } \boldsymbol{z} = (1,2,\ldots,d)^\top \in \mathbb{Z}^d.$$

Now, let the sampling nodes be given by $\boldsymbol{x}_j = j\boldsymbol{z}/(d+1) \mod 1 \in [0,1]^d$, $j = 0,\ldots,d$, then

$$\boldsymbol{k}_\ell \cdot \boldsymbol{x}_j = j\boldsymbol{k}_\ell \cdot \boldsymbol{z} = \frac{j\ell}{d+1} \mod 1$$

and thus the hyperbolic cross discrete Fourier transform

$$f_j = f(\boldsymbol{x}_j) = \sum_{\boldsymbol{k}\in H_1^d} \hat{f}_{\boldsymbol{k}} \mathrm{e}^{2\pi\mathrm{i}\boldsymbol{k}\cdot\boldsymbol{x}_j} = \sum_{\ell=0}^{d} \hat{f}_{\boldsymbol{k}_\ell} \mathrm{e}^{2\pi\mathrm{i}\frac{j\ell}{d+1}}, \qquad j = 0,\ldots,d,$$

is simply a discrete Fourier transform of length $d+1$ and can be computed in $\mathcal{O}(d\log d)$ floating point operations. In particular, the evaluation on this rank-1 lattice is, up to a constant, a unitary transform and thus numerically stable. In contrast to this it is shown in [11, Section 4] that in this special case we can evaluate the considered trigonometric polynomial at the classical sparse grid nodes in $\mathcal{O}(d)$ floating point operations but the condition number is larger than $\frac{(d-1)^2}{2}$. Moreover note that the chosen vector $\boldsymbol{z}$ is up to permutations the only possible, since its components have to be nonzero and distinct modulo $d+1$. $\square$

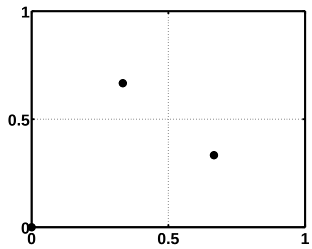

(a) $d = 2$.

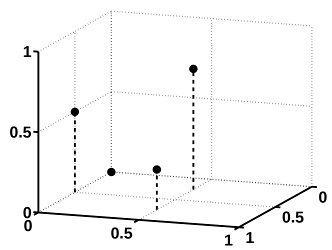

(b) $d = 3$.

Figure 3.2: Lattices for refinement $n = 1$.

Based on the "non-convexity" of the hyperbolic cross, we conclude our introductory considerations by showing that no matter what spatial discretisation is chosen, the number of sampling nodes M has to scale almost like the square of the number of Fourier coefficients $|H_n^d|$ in order to allow for orthogonal columns in the Fourier matrix.

Theorem 3.5. *Let $n, d \in \mathbb{N}$, if the Fourier matrix fulfils*

$$\boldsymbol{A}^* \boldsymbol{A} = M \boldsymbol{I} \quad \textit{then} \quad M \geq 2^{2n-2}.$$

Proof. The condition $\boldsymbol{A}^* \boldsymbol{A} = M \boldsymbol{I}$ reads as

$$\frac{1}{M} \sum_{j=0}^{M-1} \mathrm{e}^{2\pi \mathrm{i} (\boldsymbol{k}-\boldsymbol{l}) \cdot \boldsymbol{x}_j} = \delta_{\boldsymbol{k}-\boldsymbol{l}}$$

for all $\boldsymbol{k}, \boldsymbol{l} \in H_n^d$. Since $\{\boldsymbol{k}-\boldsymbol{l} : \boldsymbol{k}, \boldsymbol{l} \in H_n^d\} \supset \{\boldsymbol{k}-\boldsymbol{l} : \boldsymbol{k}, \boldsymbol{l} \in \tilde{G}_{n-1}^d\}$, $\tilde{G}_{n-1}^d = \hat{G}_{n-1}^2 \times \{0\}^{d-2}$, this implies

$$\frac{1}{M} \sum_{j=0}^{M-1} \mathrm{e}^{2\pi \mathrm{i} (\boldsymbol{k}-\boldsymbol{l}) \cdot \boldsymbol{x}_j} = \delta_{\boldsymbol{k}-\boldsymbol{l}}$$

for all $\boldsymbol{k}, \boldsymbol{l} \in \tilde{G}_{n-1}^d$. The assertion follows by reading this in matrix notation, i.e., $\tilde{\boldsymbol{A}}^* \tilde{\boldsymbol{A}} = M \boldsymbol{I}$, $\tilde{\boldsymbol{A}} = (\mathrm{e}^{2\pi \mathrm{i} \boldsymbol{k} \cdot \boldsymbol{x}_j})_{j=0,\ldots,M-1; \boldsymbol{k} \in \tilde{G}_{n-1}^d}$, for which $M \geq |\tilde{G}_{n-1}^d| = 2^{2n-2}$ is necessary. ■

3.1 Integration lattices

The hyperbolic cross can be embedded into the full d-dimensional grid, i.e., $H_n^d \subset \hat{G}_n^d$. This allows either to use the integer rank-1 lattice of size $M = 2^{dn}$ with generating vector $\boldsymbol{z} = (1, 2^n, 2^{2n}, \ldots, 2^{(d-1)n})^\top$, which is a sheared version of the full d-dimensional spatial grid G_n^d, or a slightly larger full d-dimensional spatial grid $G_{n_1} \times \ldots \times G_{n_d}$, $n \leq n_s \in \mathbb{R}$, with coprime sizes 2^{n_s}, $s = 0, \ldots, d$, which can be represented as integer rank-1 lattice as well.

Alternatively, we might use lattices for the computation of Fourier coefficients, i.e., the integration of particular trigonometric polynomials. Lattices have been intensively studied for integrating functions of many variables and integer rank-1 lattices allow for the error representation

$$\frac{1}{M} \sum_{j=0}^{M-1} f(j\boldsymbol{z}/M) - \int_{\mathbb{T}^d} f(\boldsymbol{x}) \,\mathrm{d}\boldsymbol{x} = \sum_{\substack{\boldsymbol{k} \in \mathbb{Z}^d \setminus \{\boldsymbol{0}\} \\ \boldsymbol{k} \cdot \boldsymbol{z} = 0 \mod M}} \hat{f}_{\boldsymbol{k}}$$

for $f(\boldsymbol{x}) = \sum_{\boldsymbol{k}\in\mathbb{Z}^d} \hat{f}_{\boldsymbol{k}} \mathrm{e}^{2\pi\mathrm{i}\boldsymbol{k}\cdot\boldsymbol{x}}$, see e.g. [21, Thm. 2.8]. In particular, these lattices of size M allow for the exact integration of trigonometric polynomials $f \in \tilde{\Pi}_n^{d,1}$ if and only if the vector $\boldsymbol{k}\cdot\boldsymbol{z} \neq 0 \mod M$ for $\boldsymbol{k} \in \tilde{H}_n^{d,1} \setminus \{\boldsymbol{0}\}$. In contrast, invertibility of the Fourier matrix $\boldsymbol{A}$ and thus $\boldsymbol{A}^*\boldsymbol{A} = M\boldsymbol{I}$ is equivalent to the condition that *all* numbers $\boldsymbol{k}\cdot\boldsymbol{z} \mod M$ are distinct, see Lemmata 3.1 and 3.3. Nevertheless, we might use integration lattices for the hyperbolic cross FFT as follows. The Fourier coefficients of $f(\boldsymbol{x}) = \sum_{\boldsymbol{k}\in H_n^d} \hat{f}_{\boldsymbol{k}} \mathrm{e}^{2\pi\mathrm{i}\boldsymbol{k}\cdot\boldsymbol{x}}$ are given by

$$\hat{f}_{\boldsymbol{k}} = \int_{\mathbb{T}^d} f(\boldsymbol{x})\mathrm{e}^{-2\pi\mathrm{i}\boldsymbol{k}\cdot\boldsymbol{x}}\,\mathrm{d}\boldsymbol{x}, \qquad \boldsymbol{k} \in H_n^d,$$

and they will be computed exactly if and only if the lattice rule integrates all trigonometric polynomials with Fourier coefficients supported on the difference set

$$\mathcal{H}_n^d := \{\boldsymbol{l} \in \mathbb{Z}^d : \boldsymbol{l} = \boldsymbol{k}_1 - \boldsymbol{k}_2 : \boldsymbol{k}_1, \boldsymbol{k}_2 \in H_n^d\}.$$

We easily establish the following inclusions which make known integration lattices suitable for our purpose. For the first inclusion, see also [16, Remark 1.10].

Lemma 3.6. *Let $n, d \in \mathbb{N}$ then*

$$\mathcal{H}_n^d \subset H_{2n+\min(n,d-1)}^d \quad \text{and} \quad \mathcal{H}_n^d \subset \tilde{H}_{2n-2}^{d,1},$$

and these inclusions are best possible.

Proof. For the first inclusion we consider the difference $\boldsymbol{k} - \boldsymbol{l}$ for $\boldsymbol{k}, \boldsymbol{l} \in H_n^d$. Let $\boldsymbol{u}, \boldsymbol{v} \in \mathbb{N}_0^d$ with $\|\boldsymbol{u}\|_1 \le n$, $\|\boldsymbol{v}\|_1 \le n$ and $\boldsymbol{k} \in \hat{G}_{\boldsymbol{u}}$, $\boldsymbol{l} \in \hat{G}_{\boldsymbol{v}}$ be given and set $\boldsymbol{u} = \boldsymbol{0}$ if $\boldsymbol{k} = \boldsymbol{0}$. This yields for $s = 1, \ldots, d$ the inclusions

$$k_s - l_s \in \begin{cases} \hat{G}_{u_s}, & \text{for } l_s = 0, \\ \hat{G}_{v_s+1}, & \text{for } l_s \neq 0 \text{ and } k_s = 0, \\ \hat{G}_{\max(u_s,v_s)+1} \subset \hat{G}_{u_s+v_s}, & \text{for } l_s \neq 0 \text{ and } k_s \neq 0. \end{cases}$$

Clearly $\boldsymbol{k} - \boldsymbol{l} \in \hat{G}_{\boldsymbol{j}}$ with

$$\begin{aligned} \|\boldsymbol{j}\|_1 &= \sum_{\substack{s=1\\ l_s=0}}^{d} u_s + \sum_{\substack{s=1\\ l_s\neq 0,\, k_s=0}}^{d} (v_s+1) + \sum_{\substack{s=1\\ l_s\neq 0,\, k_s\neq 0}}^{d} (u_s+v_s) \\ &\le \sum_{s=1}^{d} u_s + \sum_{s=1}^{d} v_s + |\{s \in \{1,\ldots,d\} : l_s \neq 0 \text{ and } k_s = 0\}| \\ &\le \begin{cases} \|\boldsymbol{v}\|_1 + \min(n,d), & \text{for } \boldsymbol{k} = \boldsymbol{0}, \\ \|\boldsymbol{u}\|_1 + \|\boldsymbol{v}\|_1 + \min(n,d-1), & \text{otherwise}, \end{cases} \\ &\le 2n + \min(n, d-1). \end{aligned}$$

The assertion follows from $\boldsymbol{k} - \boldsymbol{l} \in \hat{G}_{\boldsymbol{j}} \subset H_{2n+\min(n,d-1)}^d$ and this inclusion is best possible as $\boldsymbol{k} = (2^{n-1}, 0, \ldots, 0)^\top \in H_n^d$ and $\boldsymbol{l}_1 = (0, 1, \ldots, 1, 2^{n-d+1})^\top \in H_n^d$ for $d \le n$ or $\boldsymbol{l}_2 = (0, \underbrace{1, \ldots, 1}_{n \text{ times}}, 0, \ldots, 0)^\top \in H_n^d$ for $d > n$ show.

The second inclusion follows for $n=1$ from the fact that $\boldsymbol{k},\boldsymbol{l}\in H_1^d$ results in $\max(1,|k_s-l_s|)=1$, $s=1,\ldots,d$, and so $\boldsymbol{k}-\boldsymbol{l}\in\tilde{H}_0^{d,1}$. For $n>1$, Lemma 2.1 yields

$$\mathcal{H}_n^d\subset\tilde{\mathcal{H}}_n^{d,\frac{1}{2}}:=\{\boldsymbol{l}\in\mathbb{Z}^d:\boldsymbol{l}=\boldsymbol{k}_1-\boldsymbol{k}_2:\boldsymbol{k}_1,\boldsymbol{k}_2\in\tilde{H}_n^{d,\frac{1}{2}}\}$$

and we subsequently show $\tilde{\mathcal{H}}_n^{d,\frac{1}{2}}\subset\tilde{H}_{2n-2}^{d,1}$. As in the proof of Lemma 2.1, we set $\mathcal{I}_{\boldsymbol{k}}=\{s\in\{1,\ldots,d\}:k_s\neq 0\}$ and get for $\boldsymbol{k},\boldsymbol{l}\in\tilde{H}_n^{d,\frac{1}{2}}$ the estimate

$$2^{2n}\geq\prod_{s\in\mathcal{I}_{\boldsymbol{k}}}2|k_s|\prod_{s\in\mathcal{I}_{\boldsymbol{l}}}2|l_s|=2^{|\mathcal{I}_{\boldsymbol{k}}\cup\mathcal{I}_{\boldsymbol{l}}|}\prod_{s\in\mathcal{I}_{\boldsymbol{k}}\setminus\mathcal{I}_{\boldsymbol{l}}}|k_s|\prod_{s\in\mathcal{I}_{\boldsymbol{l}}\setminus\mathcal{I}_{\boldsymbol{k}}}|l_s|\prod_{s\in\mathcal{I}_{\boldsymbol{k}}\cap\mathcal{I}_{\boldsymbol{l}}}2|k_s||l_s|.$$

Together with $|k_s|,|l_s|\geq 1$ and $|k_s-l_s|\leq|k_s|+|l_s|\leq 2|k_s||l_s|$ this yields

$$\begin{aligned}2^{2n}&\geq 2^{|\mathcal{I}_{\boldsymbol{k}}\cup\mathcal{I}_{\boldsymbol{l}}|}\prod_{s\in\mathcal{I}_{\boldsymbol{k}}\setminus\mathcal{I}_{\boldsymbol{l}}}|k_s-0|\prod_{s\in\mathcal{I}_{\boldsymbol{l}}\setminus\mathcal{I}_{\boldsymbol{k}}}|0-l_s|\prod_{s\in\mathcal{I}_{\boldsymbol{k}}\cap\mathcal{I}_{\boldsymbol{l}}}\max(1,|k_s-l_s|)\\&=2^{|\mathcal{I}_{\boldsymbol{k}}\cup\mathcal{I}_{\boldsymbol{l}}|}\prod_{s=1}^{d}\max(1,|k_s-l_s|).\end{aligned}$$

Consequently, we get $\prod_{s=1}^d\max(1,|k_s-l_s|)\leq 2^{2n-|\mathcal{I}_{\boldsymbol{k}}\cup\mathcal{I}_{\boldsymbol{l}}|}$. If $|\mathcal{I}_{\boldsymbol{k}}\cup\mathcal{I}_{\boldsymbol{l}}|\geq 2$ this yields the assertion $\boldsymbol{k}-\boldsymbol{l}\in\tilde{H}_{2n-2}^{d,1}$ already. In case $|\mathcal{I}_{\boldsymbol{k}}\cup\mathcal{I}_{\boldsymbol{l}}|=1$, we have only one index $s_0\in\mathcal{I}_{\boldsymbol{k}}\cup\mathcal{I}_{\boldsymbol{l}}$ and since $|k_{s_0}|,|l_{s_0}|\leq 2^{n-1}$ and $n>1$ direct calculation shows

$$\prod_{s=1}^{d}\max(1,|k_s-l_s|)=\max(1,|k_{s_0}-l_{s_0}|)\leq 2^n\leq 2^{2n-2}.$$

Clearly, for $\boldsymbol{k}=(2^{n-1},0,\ldots,0)^\top\in H_n^d$ and $\boldsymbol{l}=(0,2^{n-1},0,\ldots,0)^\top\in H_n^d$ the difference $\boldsymbol{k}-\boldsymbol{l}$ is an element of $\tilde{H}_{2n-2}^{d,1}\setminus\tilde{H}_{2n-3}^{d,1}$. ■

3.2 Search strategies for integer rank-1 lattices

Subsequently, we sketch some strategies to find stable integer rank-1 lattices, defined by their generating vector $\boldsymbol{z}\in\mathbb{Z}^d$ and the lattice size $M\in\mathbb{N}$, algorithmically. Due to Lemmata 3.1 and 3.3, the criterion we decide on is that all entries of the vector $\boldsymbol{Hz}\mod M$ are distinct. Of course, this excludes all generating vectors where the entries of $\boldsymbol{Hz}$ are not distinct. Using additionally that the hyperbolic cross H_n^d is invariant under coordinate permutations, the entries of the generating vector can be assumed to be ordered. Possible lattice sizes M are restricted by Theorem 3.5 and the discussion in Section 3.1. Hence, a global search can be restricted to

$$\boldsymbol{z}\in\{\boldsymbol{l}\in\mathbb{N}^d:\ 0<l_1<\ldots<l_d\leq\overline{M}\},\qquad\max(2^{2n-2},|H_n^d|)\leq M<\overline{M}\leq 2^{nd},$$

where $\overline{M}$ denotes an upper bound on the lattice size, e.g., the size of a known integration lattice for trigonometric polynomials with Fourier coefficients supported on H_{2n+d-1}^d or $\tilde{H}_{2n+2}^{d,1}$, cf. Lemma 3.6. Moreover, updating the lattice size M in an outer loop, we can always restrict the entries of the generating vector to $z_1<\ldots<z_d<M$ and obtain Algorithm 1.

Algorithm 1 Lattice search, global

Input:	$n, d \in \mathbb{N}$	refinement and dimension of H_n^d, defining $\boldsymbol{H}$
	$\overline{M} \le 2^{nd}$	upper bound on the lattice size

for $M = \max(2^{2n-2}, |H_n^d|), \ldots, \overline{M}$ ***do***
  for $\boldsymbol{z} \in \{\boldsymbol{l} \in \mathbb{N}^d \,:\, 0 < l_1 < \ldots < l_d < M\}$ ***do***
    if $(\boldsymbol{H}\boldsymbol{z} \mod M)$ has distinct entries ***then***
      return $\boldsymbol{z}, M$
    end if
  end for
end for

Output:	$\boldsymbol{z} \in \mathbb{Z}^d,\ M \in \mathbb{N}$	generating vector and lattice size

3.2.1 Random generating vectors

Certainly, the global search for minimal lattices in Algorithm 1 for higher spatial dimensions or large problem sizes is not practicable. Hence, randomly chosen generating vectors are a first useful option for searching small lattices and now the inner loop runs through possible lattice sizes M. Moreover, a runtime limit seems to be an appropriate break condition for Algorithm 2.

Algorithm 2 Lattice search, random generating vector

Input:	$n, d \in \mathbb{N}$	refinement and dimension of H_n^d, defining $\boldsymbol{H}$
	$\overline{M} \le 2^{nd}$	upper bound on the lattice size
	$T > 0$	runtime limit

$M^* = \overline{M}$
while current runtime has not exceeded T ***do***
  draw $\boldsymbol{z} \in [1, M^*)^d \cap \mathbb{Z}^d$
  if $(\boldsymbol{H}\boldsymbol{z})$ has distinct entries ***then***
    for $M = \max(2^{2n-2}, |H_n^d|), \ldots, M^* - 1$ ***do***
      if $(\boldsymbol{H}\boldsymbol{z} \mod M)$ has distinct entries ***then***
        $\boldsymbol{z}^* = \boldsymbol{z},\ M^* = M,$ ***breakfor***
      end if
    end for
  end if
end while

Output:	$\boldsymbol{z}^* \in \mathbb{Z}^d,\ M^* \in \mathbb{N}$	generating vector and lattice size (if successful)

3.2.2 Generating vectors of Korobov form

Let $d, a \in \mathbb{N}$, we define the generating vector of Korobov form

$$\boldsymbol{z} = \boldsymbol{z}(a) = (1, a, a^2, \ldots, a^{d-1})^\top \in \mathbb{Z}^d,$$

which gives rise to the following result.

Lemma 3.7. *Let $d, n, a \in \mathbb{N}$, $d, n, a > 1$, and $\boldsymbol{z} = \boldsymbol{z}(a) = (1, a, \ldots, a^{d-1})^\top$ be given, then the following holds true*

i) if and only if $3 \cdot 2^{n-2} \leq a$, the vector $\boldsymbol{Hz}$ contains distinct values,

ii) if $3 \cdot 2^{n-2} \leq a \leq 2^n$ and $M < (1+a)2^{n-1}$, then $\boldsymbol{Hz} \mod M$ is not distinct,

iii) if $d = 2$, $a = 3 \cdot 2^{n-2}$, and $M = (1 + 3 \cdot 2^{n-2})2^{n-1}$, then $\boldsymbol{Hz} \mod M$ is distinct.

Proof. i) We start with dimension $d = 2$, assume $a \geq 3 \cdot 2^{n-2}$, $\boldsymbol{k}, \boldsymbol{l} \in H_n^2$, $\boldsymbol{k} \neq \boldsymbol{l}$, and show that $(\boldsymbol{k} - \boldsymbol{l}) \cdot \boldsymbol{z} = k_1 - l_1 + a(k_2 - l_2)$ is nonzero, which is trivially fulfilled for $k_2 = l_2$. In case $|k_2 - l_2| \geq 1$, we use

$$\max_{\substack{\boldsymbol{k},\boldsymbol{l} \in H_n^2 \\ k_2 \neq l_2}} |k_1 - l_1| < 3 \cdot 2^{n-2}$$

from which $(k_1 - l_1) + a(k_2 - l_2) \neq 0$ follows. For $d > 2$, the same argument yields $k_{d-1} - l_{d-1} + a(k_d - l_d) \neq 0$ and thus inductively

$$(\boldsymbol{k} - \boldsymbol{l}) \cdot \boldsymbol{z} = \sum_{j=1}^{d} a^{j-1}(k_j - l_j) = k_1 - l_1 + a(\cdots + a(k_{d-1} - l_{d-1} + a(k_d - l_d)) \cdots) \neq 0.$$

On the contrary, $a < 3 \cdot 2^{n-2}$, $\boldsymbol{k}, \boldsymbol{l} \in H_n^d$ with $k_1 - l_1 = a$, $k_2 = 0$, $l_2 = 1$, and $k_j = l_j = 0$, $j = 3, \ldots, d$, yields $\boldsymbol{k} \cdot \boldsymbol{z} = \boldsymbol{l} \cdot \boldsymbol{z}$. Moreover, this extends to $\boldsymbol{k} \cdot \boldsymbol{z}(M - a) = \boldsymbol{l} \cdot \boldsymbol{z}(M - a) \mod M$.

ii) Regarding the second assertion, let $m, r \in \mathbb{N}_0$ be chosen such that

$$M = (1 + a)2^{n-1} - 1 - s, \quad s = ma + r,\ 0 \leq m < 2^{n-1},\ 0 \leq r < a, \tag{3.3}$$

and consider $\boldsymbol{k}, \boldsymbol{l} \in H_n^d$, $\boldsymbol{k} = (-2^{n-1} + 1 + r, 0, \ldots, 0)^\top$ and $\boldsymbol{l} = (0, 2^{n-1} - m, 0, \ldots, 0)^\top$ which fulfil $\boldsymbol{k} \neq \boldsymbol{l}$ and

$$\boldsymbol{k} \cdot \boldsymbol{z} = (a + 1)2^{n-1} - 1 - ma - r - 2^{n-1} + 1 + r = a(2^{n-1} - m) = \boldsymbol{l} \cdot \boldsymbol{z} \mod M.$$

Clearly, this result remains true if $2^n < a$ under the additional assumption that M is of the particular form (3.3) with $r < 2^n$.

iii) Finally, the first assertion guarantees that the entries of $\boldsymbol{k} \cdot \boldsymbol{z}$ are distinct and since $|\boldsymbol{k} \cdot \boldsymbol{z}| < M$, we have

$$\boldsymbol{k} \cdot \boldsymbol{z} \mod M = \begin{cases} \boldsymbol{k} \cdot \boldsymbol{z} & \boldsymbol{k} \cdot \boldsymbol{z} \geq 0, \\ \boldsymbol{k} \cdot \boldsymbol{z} + M & \boldsymbol{k} \cdot \boldsymbol{z} < 0, \end{cases}$$

and thus, $\boldsymbol{k} \cdot \boldsymbol{z} = \boldsymbol{l} \cdot \boldsymbol{z} \mod M$ if and only if $\boldsymbol{k} \cdot \boldsymbol{z} \geq 0$ and $\boldsymbol{l} \cdot \boldsymbol{z} < 0$ or vice versa. We proceed by three distinct cases, where we always assume $\boldsymbol{k}, \boldsymbol{l} \in H_n^2$, $\boldsymbol{l} \cdot \boldsymbol{z} < 0$ and thus have $l_2 \leq 0$ and

$$\boldsymbol{l} \cdot \boldsymbol{z} \mod M = l_1 + l_2 \cdot 3 \cdot 2^{n-2} + (1 + 3 \cdot 2^{n-2})2^{n-1} > 2^n \quad \text{since} \quad l_2 \geq \begin{cases} -2^{n-1} + 1 & l_1 = 0, \\ -2^{n-2} + 1 & l_1 \neq 0. \end{cases}$$

The assertion follows for $\boldsymbol{k} = (k_1, 0)^\top$ with $k_1 = 0, \ldots, 2^{n-1}$ by $\boldsymbol{k} \cdot \boldsymbol{z} = k_1 \leq 2^{n-1}$, and for $\boldsymbol{k} = (k_1, 1)^\top$, $k_1 = -2^{n-2} + 1, \ldots, 2^{n-2}$, by $2^{n-1} + 1 \leq \boldsymbol{k} \cdot \boldsymbol{z} \leq 2^n$. Last but not least, let $\boldsymbol{k} = (k_1, k_2)^\top$, $k_2 = 2, \ldots, 2^{n-1}$, then $-2^{n-3} + 1 \leq k_1 \leq 2^{n-3}$ and in particular

$$\boldsymbol{k} \cdot \boldsymbol{z} \mod 3 \cdot 2^{n-2} = k_1 \mod 3 \cdot 2^{n-2} \in \{0, \ldots 2^{n-3}\} \cup \{5 \cdot 2^{n-3} + 1, \ldots, 3 \cdot 2^{n-2} - 1\}.$$

For $l_2 < 0$, we have $-2^{n-3}+1 \le l_1 \le 2^{n-3}$ and thus

$$(\boldsymbol{l}\cdot\boldsymbol{z} \mod M) \mod 3\cdot 2^{n-2} = 2^{n-1} + l_1 \in \{3\cdot 2^{n-3}+1,\ldots,5\cdot 2^{n-3}\}.$$

The only remaining case $l_2 = 0$ results in $\boldsymbol{l}\cdot\boldsymbol{z} \mod M > 3\cdot 2^{n-2}\cdot 2^{n-1} \ge \boldsymbol{k}\cdot\boldsymbol{z}$. ■

In conjunction with Theorem 3.5, the last assertion shows that for spatial dimension $d = 2$ an integer rank-1 lattice of minimal cardinality, allowing for unique and thus stable reconstruction, has size

$$2^{2n-2} \le M \le (1+3\cdot 2^{n-2})2^{n-1} \approx \frac{3}{2}2^{2n-2}.$$

We conclude this section by the following search algorithm for lattices in Korobov form.

Algorithm 3 Lattice search, Korobov form, global

Input:	$n, d \in \mathbb{N}$	refinement and dimension of H_n^d, defining $\boldsymbol{H}$
	$\overline{M} \le 2^{nd}$	upper bound on the lattice size

$M^* = \overline{M}$
for $a = 3\cdot 2^{n-2},\ldots,M^*-3\cdot 2^{n-2}$ ***do***
  for $M = \max(2^{2n-2},|H_n^d|),\ldots,M^*-1$ ***do***
    if condition (3.3) is not fulfilled ***then***
      $\boldsymbol{z} = (1,a,\ldots,a^{d-1})^\top$
      if $(\boldsymbol{H}\boldsymbol{z} \mod M)$ has distinct entries ***then***
        $\boldsymbol{z}^* = \boldsymbol{z}$, $M^* = M$, ***breakfor***
      end if
    end if
  end for
end for

Output:	$\boldsymbol{z}^* \in \mathbb{Z}^d$, $M^* \in \mathbb{N}$	generating vector and lattice size

4 Numerics

Subsequently, we search for stable lattices of small cardinality by different strategies, compare these discretisations to integration lattices, and finally perform CPU timings for the different variants of the hyperbolic cross discrete Fourier transform. Following the commonly accepted concept of *reproducible research*, all numerical experiments are included in our publicly available toolbox [5]. The numerical results were obtained on an Intel Core i7 CPU 920 with 2.67GHz, 12GByte RAM running OpenSUSE Linux 11.1 X86_64 and Matlab 7.10.0.499. Time measurements were performed by employing the Matlab function `cputime`.

4.1 Finding new lattices

Integer lattices of small cardinality can be found by Algorithms 1 - 3 and variants thereof. Table 4.1 summarises these efforts for spatial dimensions $d = 2, 3, 6, 10$. The problem size is given by the refinement n and by the cardinality of the hyperbolic cross H_n^d in the first two columns, respectively. The output of Algorithm 1 is denoted by M_{glob} and we stopped this global search subsequent to the refinement that exceeded 100 seconds for testing, except for $d = 10$ where already $n = 2$ results in quite large response times. Algorithm 2 utilises randomisation for finding lattices of size M_{rand} as given in the fourth column of Table 4.1. Here, we set the runtime limit to $T = 100$ seconds and the fifth column presents the number of tested random vectors denoted by $\#\boldsymbol{z}$. We discussed generating vectors of Korobov form in Section 3.2.2. The results of Algorithm 3 are shown in column M_{kor}. Similar to Algorithm 2, a randomised version generates the parameter a at random and the found lattice sizes are reported in column $M_{\text{kor,rand}}$. Finally, the last column labeled by $M_{\text{kor},3\cdot 2^{n-2}}$, shows the minimal lattice size for the vector $\boldsymbol{z}(3 \cdot 2^{n-2})$.

In comparison with global search strategies, randomisation for generating the whole vector $\boldsymbol{z} \in \mathbb{Z}^d$ or the parameter a for vectors of Korobov form seems a reasonable choice. Additionally, one might reduce search time by fixing the parameter to $a = 3 \cdot 2^{n-2}$ at the cost of a further increase of the lattice size M.

n	$\lvert H_n^2\rvert$	M_{glob}	M_{rand}	$\#\boldsymbol{z}$	M_{kor}	$M_{\text{kor,rand}}$	$\#\boldsymbol{z}$	$M_{\text{kor},3\cdot 2^{n-2}}$
2	8	8	8	2312909	8	8	2312046	8
3	20	28	28	840019	28	28	769916	28
4	48	93	93	181096	93	93	167254	104
5	112	314	314	27903	314	314	28064	400
6	256	1167	1167	3584	1167	1167	3709	1568
7	576	-	4473	416	4443	4461	449	6208
8	1280	-	17517	47	-	17330	52	24704
9	2816	-	68595	6	-	68332	6	98560
10	6144	-	269712	1	-	272837	1	393728
11	13312	-	1079129	1	-	1067797	1	1573888
n	$\lvert H_n^3\rvert$	M_{glob}	M_{rand}	$\#\boldsymbol{z}$	M_{kor}	$M_{\text{kor,rand}}$	$\#\boldsymbol{z}$	$M_{\text{kor},3\cdot 2^{n-2}}$
2	13	14	14	1160436	14	14	1205784	20
3	38	52	52	232561	52	52	247791	82
4	104	198	198	30465	213	213	30837	247
5	272	-	781	3511	819	819	3679	946
6	688	-	3391	356	3052	3302	380	5145
7	1696	-	14973	35	-	14678	38	16822
8	4096	-	60426	4	-	65724	4	56905
9	9728	-	294533	1	-	243813	1	248611
n	$\lvert H_n^6\rvert$	M_{glob}	M_{rand}	$\#\boldsymbol{z}$	M_{kor}	$M_{\text{kor,rand}}$	$\#\boldsymbol{z}$	$M_{\text{kor},3\cdot 2^{n-2}}$
2	34	50	52	161804	59	59	228449	92
3	138	-	418	9077	351	351	12778	551
4	501	-	2818	452	1736	2072	581	3346
5	1683	-	23040	22	-	17444	28	20486
6	5336	-	159227	2	-	121295	2	138770
7	16172	-	930342	1	-	728406	1	743759
n	$\lvert H_n^{10}\rvert$	M_{glob}	M_{rand}	$\#\boldsymbol{z}$	M_{kor}	$M_{\text{kor,rand}}$	$\#\boldsymbol{z}$	$M_{\text{kor},3\cdot 2^{n-2}}$
2	76	-	211	22398	197	197	39905	281
3	416	-	3844	434	1661	1661	784	3661
4	1966	-	52364	9	13237	33959	12	35873
5	8378	-	590791	1	-	283487	1	296609

Table 4.1: Interpolation lattices for the dyadic hyperbolic cross H_n^d and spatial dimensions $d = 2, 3, 6, 10$.

4.2 Integration lattices

For the two-dimensional case $d = 2$, Lemma 3.7 iii) assures an interpolation lattice of size $M = (1 + 3 \cdot 2^{n-2}) \cdot 2^{n-1} \approx \frac{3}{4} 2^{2n-1}$ and this cardinality can be further reduced numerically, cf. Table 4.1. In contrast, we might use that the ℓ^1 ball is the smallest "convex" set containing the hyperbolic cross and employ the *minimal* integration lattices from [4, Theorems 2.4 and 6.1]. These integrate trigonometric polynomials with total degree $\|\boldsymbol{k}\|_1 = |k_1| + |k_2| \leq 2^n - 1$ exactly and thus allow for the stable reconstruction of $f \in \Pi_n^2$ using $M = 2^{2n-1}$ nodes.

More general, we outlined the use of integration lattices for the reconstruction problem in Section 3.1. Using the inclusions of Lemma 3.6, we compare our numerically found lattices to lattices which integrate trigonometric polynomials with Fourier coefficients supported on sufficiently large Zaremba crosses exactly. As usual, we associate to a given integer lattice $\mathcal{X} \subset \mathbb{T}^d$ the Zaremba index and the corresponding refinement

$$\varrho = \varrho(\mathcal{X}) = \min_{\substack{\boldsymbol{k} \in \mathbb{Z}^d \setminus \boldsymbol{0} \\ \boldsymbol{k} \cdot \boldsymbol{z} = 0 \mod M}} \left(\prod_{s=1}^{d} \max(1, |k_s|) \right), \quad n(\varrho) = \left\lfloor \frac{\log_2(\varrho - 1)}{2} \right\rfloor + 1$$

such that Lemma 3.6 assures that trigonometric polynomials $f \in \Pi_{n(\varrho)}$, will be reconstructed in a stable way from its samples.

Lattices for the integration of functions of dominating mixed smoothness have been considered by several authors and the optimality criterion is the quadrature error, cf. [8], or an estimate on it based on the Zaremba index, cf. [12, 17, 15]. More specific, we consider rank-1 lattices from [12, 17] for $d = 3$ and rank-1 lattices with generating vectors of Korobov form [8] for $d = 3, 6$. Table 4.2 compares these integration lattices and the smallest interpolation lattices from Section 4.1 with respect to the Zaremba index ϱ, the corresponding refinement $n(\varrho)$ which assures stable reconstruction by Lemma 3.6, and the largest refinement n which allows for stable reconstruction by Lemma 3.1. As can readily be seen, the newly found lattices allow for the stable reconstruction of trigonometric polynomials $f \in \Pi_n^d$ while having only a relatively small Zaremba index.

4.3 Computational times

Subsequently, we compare the CPU timings of the lattice based hyperbolic cross fast Fourier transform (LHCFFT), see Equation (3.1), the hyperbolic cross fast Fourier transform (HCFFT), implemented in [5], and the straightforward computation, denoted by hyperbolic cross discrete Fourier transform (HCDFT). The LHCFFT uses the generating vector $\boldsymbol{z}(3 \cdot 2^{2n-2}) \in \mathbb{Z}^d$ and the lattice size M is the minimal possible as partially reported in the last column of Table 4.1. For fixed spatial dimensions $d = 2, 3, 6, 10$, Figure 4.1 considers CPU timings with respect to increasing refinement n. While the asymptotic complexity of the LHCFFT, $\Omega(4^n n)$, is larger than for the HCFFT, $\mathcal{O}(2^n n^d)$, we nevertheless gain at least one order of magnitude in the absolute computational times for problems of moderate size. On the other hand, we consider fixed refinements $n = 2, 3, 4, 5$ and increasing spatial dimension in Figure 4.2. Here, the problem size is $|H_n^d| = \mathcal{O}(d^n)$ and the asymptotic complexities are $\mathcal{O}(d^{n+1})$ for the HCFFT and $\mathcal{O}(d^{2n})$ for the HCDFT. Regarding the LHCFFT, we cannot offer any meaningful bound for its complexity but gain at least one order of magnitude in the absolute computational times as above.

	M	ϱ	$n(\varrho)$	n
[8]	512	30	3	4
	2048	90	4	4
	4096	126	4	5
	8192	286	5	5
	12288	285	5	6
	49152	950	5	7
	65536	1320	6	7
[12]	2120	165	4	5
	3336	258	5	5
	5364	404	5	6
[17]	4002	280	5	5
	6066	460	5	6
	16914	1120	6	6
	54525	2904	6	7
	109050	5310	7	7
	120660	5370	7	8
Table 4.1	198	15	2	4
	781	25	3	5
	3052	110	4	6
	14678	384	5	7
	56905	192	4	8

(a) $d = 3$.

	M	ϱ	$n(\varrho)$	n
[8]	1024	4	1	2
	4096	9	2	3
	24576	15	2	4
	32768	30	3	4
	49152	36	3	4
	65536	42	3	5
Table 4.1	50	1	0	2
	351	1	0	3
	1736	6	2	4
	17444	12	2	5

(b) $d = 6$.

Table 4.2: Comparison of interpolation lattices for the dyadic hyperbolic cross H_n^d and integration lattices for the Zaremba cross $\tilde{H}_{2n-2}^{d,1}$.

5 Summary

The evaluation of a d-variate trigonometric polynomial on an integer rank-1 lattice reduces to a single one dimensional FFT. Provided the integer rank-1 lattice allows for unique and thus stable reconstruction, for which Theorem 3.5 makes a strong oversampling necessary, the same holds true for the computation of Fourier coefficients from samples on that lattice. Besides the availability of highly efficient implementations for the standard FFT, this completely cures the numerical instabilities [11] of the somewhat more involved standard sparse grid discretisation [1, 9, 7]. We proposed several algorithms for searching small integer rank-1 lattices, reported their size in Table 4.1, and showed their use for computing discrete Fourier transforms. In particular, this lattice based hyperbolic cross fast Fourier transform is available in [5] and outperforms known algorithms by at least one order of magnitude with respect to CPU timings for moderate problem sizes. While integer rank-1 lattices prove useful in practice, we could not prove useful upper bounds for their minimal cardinality.

Acknowledgement

The authors gratefully acknowledge support by the German Research Foundation within the project KU 2557/1-1 and by the Helmholtz Association within the young investigator group VH-NG-526.

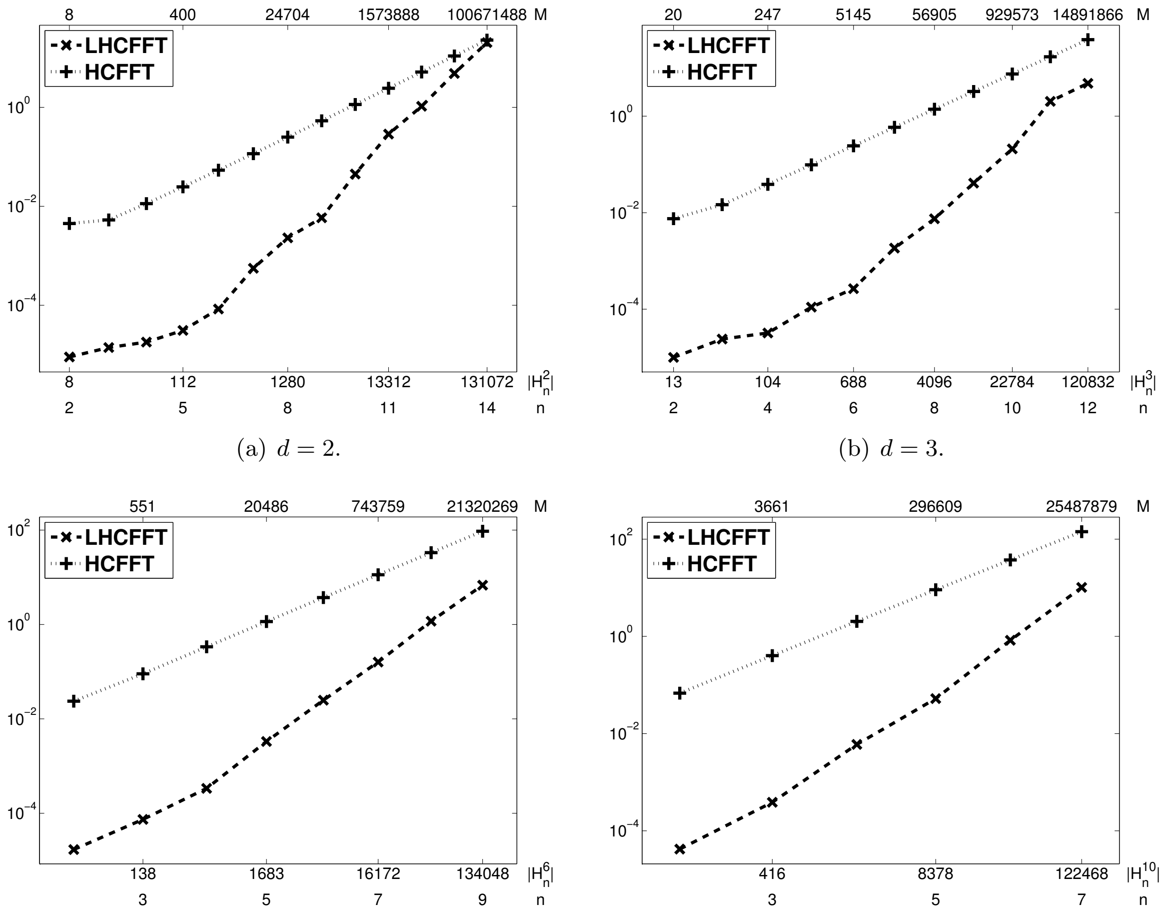

(a) $d = 2$. (b) $d = 3$.

(c) $d = 6$. (d) $d = 10$.

Figure 4.1: Computational times in seconds of the hyperbolic cross discrete Fourier transforms with respect to the refinement n, the problem size $|H_n^d|$, and the used lattice size M for fixed spatial dimensions $d = 2, 3, 6, 10$.

References

[1] G. Baszenski and F.-J. Delvos. A discrete Fourier transform scheme for Boolean sums of trigonometric operators. In C. K. Chui, W. Schempp, and K. Zeller, editors, *Multivariate Approximation Theory IV*, ISNM 90, pages 15 – 24. Birkhäuser, Basel, 1989.

[2] H.-J. Bungartz and M. Griebel. Sparse grids. *Acta Numer.*, 13:147 – 269, 2004.

[3] R. Cools, F. Y. Kuo, and D. Nuyens. Constructing lattice rules based on weighted degree of exactness and worst case error. *Computing*, 87:63–89, 2010.

[4] R. Cools and I. H. Sloan. Minimal cubature formulae of trigonometric degree. *Math. Comp.*, 65(216):1583–1600, 1996.

[5] M. Döhler, L. Kämmerer, S. Kunis, and D. Potts. NHCFFT, Matlab toolbox for the nonequispaced hyperbolic cross FFT. `http://www.tu-chemnitz.de/~skunis/software.php`, 2009.

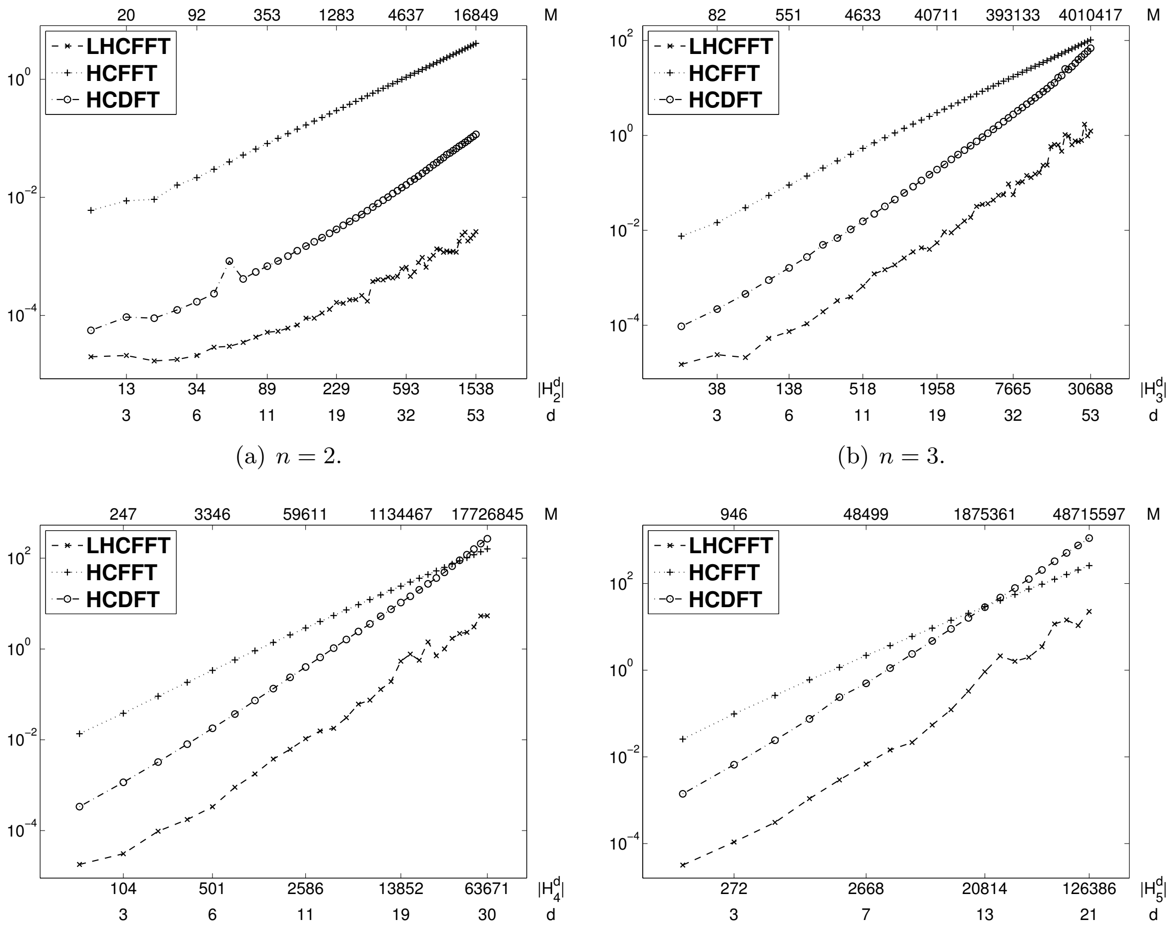

(a) $n = 2$.

(b) $n = 3$.

(c) $n = 4$.

(d) $n = 5$.

Figure 4.2: Computational times in seconds of the hyperbolic cross discrete Fourier transforms with respect to the spatial dimension d, the problem size $|H_n^d|$, and the used lattice size M for fixed refinements $n = 2, 3, 4, 5$.

[6] M. Döhler, S. Kunis, and D. Potts. Nonequispaced hyperbolic cross fast Fourier transform. *SIAM J. Numer. Anal.*, 47:4415 – 4428, 2010.

[7] V. Gradinaru. Fourier transform on sparse grids: Code design and the time dependent Schrödinger equation. *Computing*, 80:1 – 22, 2007.

[8] S. Haber. Parameters for integrating periodic functions of several variables. *Math. Comp.*, 41(163):115–129, 1983.

[9] K. Hallatschek. Fouriertransformation auf dünnen Gittern mit hierarchischen Basen. *Numer. Math.*, 63:83 – 97, 1992.

[10] Y. Jiang and Y. Xu. Fast discrete algorithms for sparse Fourier expansions of high dimensional functions. *J. Complexity*, 26:51–81, 2010.

[11] L. Kämmerer and S. Kunis. On the stability of the hyperbolic cross discrete Fourier transform. *Numer. Math.*, accepted.

[12] G. Kedem and S. K. Zaremba. A table of good lattice points in three dimensions. *Numer. Math.*, 23:175–180, 1974.

[13] J. Keiner, S. Kunis, and D. Potts. Using NFFT3 - a software library for various nonequispaced fast Fourier transforms. *ACM Trans. Math. Software*, 36:Article 19, 1 – 30, 2009.

[14] F. Y. Kuo, I. H. Sloan, and H. Woźniakowski. Lattice rules for multivariate approximation in the worst case setting. In *Monte Carlo and quasi-Monte Carlo methods 2004*, pages 289–330. Springer, Berlin, 2006.

[15] T. N. Langtry. Lattice rules of minimal and maximal rank with good figures of merit. *J. Comput. Appl. Math.*, 112(1-2):147–164, 1999. Numerical evaluation of integrals.

[16] C. Lubich. *From quantum to classical molecular dynamics: reduced models and numerical analysis*. Zurich Lectures in Advanced Mathematics. European Mathematical Society (EMS), Zürich, 2008.

[17] J. N. Lyness and T. Sørevik. Lattice rules by component scaling. *Math. Comp.*, 61(204):799–820, 1993.

[18] W. Sickel and F. Sprengel. Interpolation on sparse grids and tensor products of Nikol'skij-Besov spaces. *J. Comput. Anal. Appl.*, 1:263 – 288, 1999.

[19] W. Sickel and F. Sprengel. Some error estimates for periodic interpolation of functions from Besov spaces. In W. Haussman, K. Jetter, and M. Reimer, editors, *Advances in multivariate approximation*, pages 269 – 287. Wiley-VCH, 1999.

[20] W. Sickel and T. Ullrich. The Smolyak algorithm, sampling on sparse grids and function spaces of dominating mixed smoothness. *East J. Approx.*, 13:387 – 425, 2007.

[21] I. H. Sloan and S. Joe. *Lattice methods for multiple integration*. Oxford Science Publications. The Clarendon Press Oxford University Press, New York, 1994.

[22] F. Sprengel. A class of function spaces and interpolation on sparse grids. *Numer. Funct. Anal. Optim.*, 21:273 – 293, 2000.

[23] V. N. Temlyakov. Approximation of functions with bounded mixed derivative. *Proc. Steklov Inst. Math.*, pages vi+121, 1989. A translation of Trudy Mat. Inst. Steklov 178 (1986).

[24] T. Ullrich. Smolyak's algorithm, sampling on sparse grids and Sobolev spaces of dominating mixed smoothness. *East J. Approx.*, 14:1 – 38, 2008.

[25] S. K. Zaremba. La méthode des "bons treillis" pour le calcul des intégrales multiples. In *Applications of number theory to numerical analysis (Proc. Sympos., Univ. Montreal, Montreal, Que., 1971)*, pages 39–119. Academic Press, New York, 1972.

[26] C. Zenger. Sparse grids. In *Parallel algorithms for partial differential equations (Kiel, 1990)*, volume 31 of *Notes Numer. Fluid Mech.*, pages 241 – 251. Vieweg, Braunschweig, Germany, 1991.